4.3.6 Interplanetary particles and magnetic fields

BERNDT KLECKER

4.3.6.1 Interplanetary plasma and magnetic field (solar wind)

More than five decades of active research with various spaceprobes cruising through the inner and outer heliosphere resulted in a wealth of measurements of solar wind parameters throughout the heliosphere [90S, 01N, 03N]. The Helios probes collected data in the distance range between 0.29 AU and 1 AU for more than 12 years [b, c]. The Pioneer 10/11 and the Voyager 1/2 spaceprobes were exploring the outer heliosphere [a, 77S, 84B1, 84B2, 84G, 03R] where Voyager 1 and Voyager 2 crossed the termination shock at a distance of 94 AU in 2004 and 2007, respectively [05S]. The Ulysses spacecraft has orbited the Sun in a polar orbit measuring solar wind plasma and magnetic field from the ecliptic to high latitudes, both for solar minimum and solar maximum conditions [91B, 00M, 01N, 03M].

These measurements showed that there are several types of solar wind:

1. The fast-type solar wind usually found in high-speed streams emerges from coronal holes which are representative of the inactive sun. At times around minimum solar activity large coronal holes cover both polar caps of the sun, with occasional extension down to the equatorial regions (see Fig. 1). The plasma properties remain fairly steady throughout a high speed stream and do not vary much between different fast streams [b, c, d, 90S, 00M].
2. The slow solar wind of the interstream type is also typical of times around minimum solar activity. Its sources are constrained to the warped activity belt of about 40° in latitude which encircles the sun close to the equator, thus separating the polar coronal holes from each other. This is the regime of bright coronal streamers. The strikingly low helium content (< 2%) indicates a larger release height in the gravitationally stratified solar atmosphere [b, c, d, 90S].
3. The slow solar wind of the maximum type is found to emerge at high solar activity from substantially larger areas often located far from coronal streamers. It is highly variable and usually contains a significant fraction of helium (some 4%), indicating a release at lower altitudes in the corona. Otherwise, the properties are similar to the interstream-type solar wind [b, c, d, 90S].
4. The coronal mass ejections (CME) in conjunction with transient events in the corona may exhibit some (but not necessarily all) of the following signatures: significant increase of the helium content (up to 40%), occurrence of a large fraction of Fe^{16+} and He^{+} ions, depressions of ion and electron temperatures, bi-directional streaming of electrons and suprathermal ions, high magnetic field strength with low variance, very low plasma beta, and large scale rotation of the magnetic field vector indicating the occurrence of magnetic clouds [e, 01F].

The basic properties of the first three types of solar wind as determined in the ecliptic and at high solar latitudes are compiled in Table 1. The data in Table 1 are compiled from various references. The data inside 1 AU were collected by the two Helios solar probes between December 1974 and December 1976, covering radial distances of 0.3 to 1 AU. All parameters involving the proton density n_p were normalized to 1 AU assuming a r^{-2} dependence. Only those temperature data obtained between 0.9 and 1 AU were included. The 1 AU data (from the IMP satellites) are taken from a collection of solar wind parameters [77F] compiled in [90S]. The Helios and Ulysses data were taken from various references as indicated in the table.

Magnetic field and mixed parameters are summarized in Table 2. In the inner heliosphere (Helios data), the radial dependence of the magnetic field strength and its vector components on distance r [AU] from the Sun is given in the form $B(r) \sim r^{\alpha}$ [90M]. In the near ecliptic outer heliosphere (Voyager 1/2) the magnetic field was fitted assuming a Parker spiral shape $B_P = B_0\, r^{-2} \sqrt{(1+r^2)}$, with r in units of AU [84B1]. The radial and latitudinal dependence of the solar wind parameters as obtained with Ulysses have been separated by a least square fit to the solar wind parameter Y assuming $Y = R^{\alpha} (Y_0 + b\ \theta)$ [00M]. Columns 7 and 8 of Table 1 and columns 7, 8 and 9 of Table 2 show the statistical properties of the high-latitude solar wind (above 36° latitude), scaled to a distance of 1 AU, and the radial and latitudinal depence, respectively. The small value of b in column 9 of Table 2 shows that the latitudinal dependence of the solar wind parameters is very small [90M, 01S].

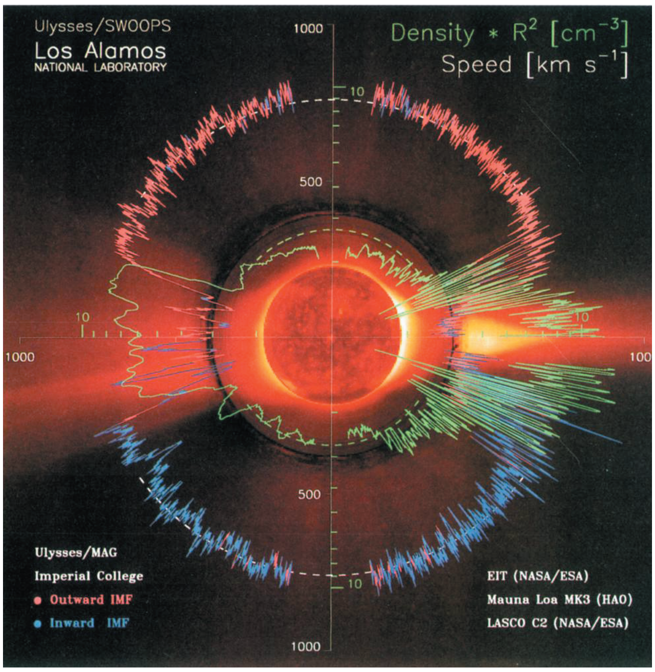

Fig. 1 (see color-picture part, page 628). Summary plot of the first orbit of Ulysses over the poles of the Sun. The solar wind proton density (green trace) shows a one solar rotation running average. The red and blue traces show one hour averages of the solar wind speed for outward (red) and inward (blue) interplanetary magnetic field, respectively [00M].

In the inner heliosphere where the solar wind is streaming off freely, the actual profiles depend on the type of solar wind [90P, 90S, 91M]. With increasing distance from the Sun solar wind streams of different speeds interact with each other. Finally, all solar wind plasma will have been processed by stream-stream interactions. Thus, in the outer heliosphere the original signatures are lost [84B2, 92G].

New observations with advanced instrumentation onboard Earth-orbiting satellites and spaceprobes, in particular with coronographs, EUV-telescopes and much improved sensors for in-situ measurements, dramatically improved the diagnostics of transient phenomena in the solar wind. There are now observations of coronal mass ejections (CMEs) and their interplanetary counterparts (ICMEs) over several solar cycles [e, 87K, 92J, 06G, 06S]. The CMEs and ICMEs, depending on their scale and speed, may drive coronal and interplanetary shock waves through the ambient solar wind that in turn may accelerate ions and electrons to high energies (see also 4.3.6.2.1) [e, 86S, 06G, 06S].

Definition of the solar wind parameters of Table 1 and Table 2:

v_p			proton bulk speed
n_p			proton density
F_p	=	$n_p v_p$	proton flux density
M_p	=	$n_p m_p v_p^2$	proton momentum flux density
n_p / n_α			α-particle density ratio
E_k	=	$1/2\ n_p m_p v_p^3$	kinetic energy flux density
E_g	=	$n_p v_p G\ m_p\ M_s/R_s$	potential energy flux density
E_{thp}	=	$5/2\ n_p v_p k\ T_p$	proton enthalpy flux density
E_{the}	=	$5/2\ n_e v_e k\ T_e$	electron enthalpy flux density
Q_e			electron heat flux density
Q_p			proton heat flux density
E_A			Alfvén wave energy flux density
E_t	=	$E_k + E_g$	total energy flux density
T_p			proton temperature

$A_{Tp} = T_{p\perp} / T_{p\parallel}$	proton temperature anisotropy
T_e	electron temperature
$A_{Te} = T_{e\perp} / T_{e\parallel}$	electron temperature anisotropy
T_α	α-particle temperature
$A_{T\alpha} = T_{\alpha\perp} / T_{\alpha\parallel}$	α-particle temperature anisotropy
T_α/T_p	helium ion to proton temperature ratio
L_p	angular momentum flux (particles)
L_m	angular momentum flux (magnetic field)
$\|B\|$	magnetic field strength
$\|B_r\|$	magnetic field, radial component
$\|B_\theta\|$	magnetic field, out-of-ecliptic component
B_ϕ	magnetic field, azimuthal component
$\beta_{ion} = P_{ion} / P_B$	plasma pressure / magnetic field pressure
$V_A \sim \|B\|/n^{1/2}$	Alfvén velocity
$M_A = v_p / V_A$	Alfvénic mach number

Table 1. Average values of solar wind parameters at 1 AU, and at high solar latitudes. The data were compiled from various references. The 1 AU data (from the IMP satellites) are taken from the compilation in [90S] that is based on a collection of solar wind parameters in [77F]. The Helios and Ulysses data were taken from various references as indicated in the table.

Plasma parameters[1]		Slow wind		Fast wind			High latitude[*] (above 36° Lat)		
		Helios	1 AU	Helios	1 AU	Ref.	Ulysses	α	Ref.
v_p	[km s^{-1}]	348	327	667	702	83S	758.	0	00M
n_p	[cm^{-3}]	10.7	8.3	3.0	2.73	83S	2.7	–2	00M
F_p	[10^8 cm^{-2} s^{-1}]	3.66	2.7	1.99	1.9	83S	2.4	–2	00M
M_p	[10^8 dyn cm^{-2}]	2.12		2.26		83S			
n_α/n_p		0.025	0.038	0.036	0.048	83S	0.044		00M
E_k	[erg cm^{-2} s^{-1}]	0.37	0.25	0.76	0.79	83S			
E_g	[erg cm^{-2} s^{-1}]	1.17	0.87	0.65	0.60	83S			
E_{thp}	[10^{-3} erg cm^{-2} s^{-1}]	11	3.0	23	16	83S			
E_{the}	[10^{-3} erg cm^{-2} s^{-1}]		11		7	83S			
Q_e	[10^{-3} erg cm^{-2} s^{-1}]	6.0	2.7	8.0	2.2	90P	7.4	–2.9	01S
Q_p	[10^{-3} erg cm^{-2} s^{-1}]	0.08	0.029	0.3	0.16	84M			
E_A	[10^{-3} erg cm^{-2} s^{-1}]		0.7	14	6.7	83S			
E_t	[erg cm^{-2} s^{-1}]	1.55	1.18	1.43	1.51	83S			
T_p	[10^3 K]	55	34	280	230	82M1	270	–1.02	00M
A_{Tp}		1.7		1.2		82M1			
T_e	[10^3 K]	190	130	130	100	90P			
A_{Te}		1.2		1.6		90P			
T_α	[10^3 K]	170	110	730	1420	82M2	1400	–0.8	00M
$A_{T\alpha}$		1.4		1.3		82M2			
T_α/T_p		2.9	3.2	3.0	6.2	82M2			
L_p	[10^{30} dyn cm sr^{-1}]	2.14		–0.56		83P			
L_m	[10^{30} dyn cm sr^{-1}]	0.14		0.15		83P			

[1]: definitions see below. [*]:Radial dependence $\sim r^\alpha$

Table 2. Average values of magnetic field and plasma parameters

Magnetic field parameters[1]		Low latitude wind**					High latitude fast wind**			
		Slow wind		Fast wind			$Y = r^{\alpha}(Y_0 + b\theta)$			
		B_0	α	B_0	α	Ref	Y_0	α	b	Ref
$\|B\|$	[nT] (0.3 - 1.0 AU)	3.45	−1.64	3.28	−1.86	90M	5.61	−1.47	−0.0161	00M
$\|B_r\|$	[nT]	2.47	−2.02	2.77	−1.97	90M	3.36	−1.77	−0.00974	00M
B_θ	[nT]	1.95	−1.32	1.44	−1.34	90M				00M
B_ϕ	[nT]	2.96	−1.07	2.19	−1.13	90M				00M
$\|B_P\|$	[nT] (1-10 AU)	4.5				84B1				
β_{ion}							1.05	0.11	0.0041	00M
V_A	[km s^{-1}]						64.9	−0.49	−0.087	00M
M_A							11.4	0.49	0.0289	00M

[1] Definitions see below; (*) $B_i \sim r^{\alpha}$; (**) 1 AU scaled mean, with $Y = r^{\alpha}(Y_0 + b\theta)$, where r is the radial distance from the Sun in AU and θ is the solar latitude, with $\theta = 0$ in the ecliptic [00M];

Table 3 summarizes typical properties and statistics of coronal mass ejections (CMEs) and Interplanetary Coronal Mass Ejections (ICMEs) as obtained in solar cycles 21 and 23. The differences between the two solar cycles are partly due to the higher sensitivity of the recent measurements and partly due to differences in the solar cycles [06S, 06G]. The relation between solar flares and CMEs is still under investigation. There is evidence that flares and CMEs are consequences of a more fundamental process resulting in a large scale restructuring of the magnetic field at the Sun [00F, 02P, 06H].

Table 3. Average properties of Coronal Mass Ejections

	Solar Cycle 21 1979 - 1981 998 CMEs (SOLWIND)			Solar Cycle 23 1996 - 2003 ~9000 CMEs (SOHO)		
	Average	Range	Ref	Average	Range	Ref
Speed [km s^{-1}]	470	<50 … 1680	85H	483	~100 … 3000	06G
Total ejected mass [g]	$4.1\ 10^{15}$	$2\cdot10^{14}$ … $4\cdot10^{16}$	85H	$6.7\ 10^{14}$	~10^{13} … 10^{16}	06G
Total kinetic energy [erg]	$3.5\ 10^{30}$	<10^{29} … $6\cdot10^{31}$	85H	$5.4\ 10^{29}$	~10^{27} … 10^{33}	06G
Angular span [°]	45	~2 … 360	85H	46	<10 … 360	06G
Average rate (sol max) [day^{-1}]	1.8		85H	~6		06G
Average rate (sol min) [day^{-1}]				0.5		06G

References for 4.3.6.1

General references

a Physics of the Outer Heliosphere (Grzedzielski, S., Page, D.E., eds). COSPAR Colloquia Series 1 (1990)

b Physics of the Inner Heliosphere, I. Large-Scale Phenomena (Schwenn, R., Marsch, E., eds.), Berlin, Springer Verlag (1990).

c Physics of the Inner Heliosphere, II. Particles, Waves, and Turbulence (Schwenn, R., Marsch, E., eds.), Berlin, Springer Verlag (1991).

d The Heliosphere Near Solar Minimum, The Ulysses Perspective (Balogh, A., Marsden, R.G., Smith. E.J., eds.) Springer (2001).

e Coronal Mass Ejections, (Kunow, H., Crooker, N.U., Linker, J.A., Schwenn, R., von Steiger, R. eds.), Space Science Reviews 123, No 1-3 (2006).

Special references

77F Feldman, W.C., in: The solar output and its variations (White, O.R., ed). Boulder, Co, USA: Colorado Associated University Press (1977) 351.
77S Stone, E.C.: Space Science Rev. **21(2)** (1977) 75.
82M1 Marsch, E., Mühlhäuser, K.-H., Schwenn, R., et al.: J. Geophys. Res. **87** (1982) 52.
82M2 Marsch, E., Mühlhäuser, K.-H., Rosenbauer, H., et al.: J. Geophys. Res. **87** (1982) 35.
83P Pizzo, V., Schwenn, R., Marsch, E., et al.: Astrophys. J. **271** (1983) 335.
83S Schwenn, R.: in: Solar Wind Five (Neugebauer, M., ed), NASA Conf. Publ. 2280, Pasadena, Ca, USA (1983) 489.
84B1 Burlaga, L.F., Klein, L.W., Lepping, R.P., Behannon, K.W.: J. Geophys. Res. **89** (1984) 10659.
84B2 Burlaga, L.F.: Space Sci. Rev. **39** (1984) 255.
84G Gazis, P.R.: J. Geophys. Res. **89** (1984) 775.
84M Marsch, E., Richter, A.K.: J. Geophys. Res. **89** (1984) 6599.
85H Howard, R.A., Sheeley, jr., N.R., Koomen, M.J., Michels, D.J.: J. Geophys. Res. **90** (1985) 8173.
86S Schwenn, R.: Space Sci. Rev. **44** (1986) 139.
87K Kahler, S.: Rev. Geophys. **25** (1987) 663.
90M Mariani, F., Neugebauer, F.M.: see General references [b] p. 183.
90P Pilipp, W.G., Miggenrieder, H., Mühlhäuser, K.-H., et al.: J. Geophys. Res. **95** (1990) 6305.
90S Schwenn, R.: see General references [b] p. 99.
91B Burlaga, L.F.: see General references [c] p. 1.
91M Marsch, E.: see General References [c] p. 45.
92G Gazis, P.R., Barnes, A., Mihalov, J.D., Lazarus, A.J., in : Solar Wind Seven, COSPAR Colloquia Series 3 (Marsch, E., Schwenn, R, eds.), Oxford: Pergamon Press (1992) 179.
92J Jackson, B.V., in: Solar Wind Seven, COSPAR Colloquia Series 3 (Marsch, E., Schwenn, R, eds.), Oxford: Pergamon Press (1992) 623.
00F Forbes, T.G.: J. Geophys. Res. **105** (2000) 23153.
00M McComas, D.J., Barraclough, B.L., Funsten, H.O., et al.: J. Geophys. Res. **105** (2000) 10419.
01F Forsyth, R.J., Gosling, J. T.: see General references [d] p. 107.
01N Neugebauer, M.: see General references [d] p. 43.
01S Scime, E.E., Littleton, J.E.: Geophys. Res. Lett. **28** (2001) 2169.
02P Priest, E.R., Forbes, T.G.: Astron. Astrophys. Rev. **10** (2002) 313.
03M McComas, D.J., in: Solar Wind 10, Proc. Tenth International Solar Wind Conf., AIP Conf. Proc. **679** (2003), p 33.
03N Neugebauer, M., in: Solar Wind 10, Proc. Tenth International Solar Wind Conf., AIP Conf. Proc. **679** (2003), p 8.
03R Richardson, J.D., Wang, C., Burlaga, L.F.: Geophys. Res. Lett. **30** (2003) SSC 6-1.
05S Stone, E.C., Cummings, E.C., McDonald, F.B., Heikkila, B.C., Lal, N., Webber, W.R.: Science **309** (2005) 2017.
06G Gopalswamy, N.: J. Astrophys. Astr. **27** (2006) 243.
06H Harrison, R., in: Solar Eruptions and Energetic Particles (Gopalswamy, N., Mewaldt, R.A., Torsti, J., eds.), Geophysical Monograph Series 165, American Geophysical Union (2006), p 73.
06S Schwenn, R., Raymond, J. C., Alexander, D., et al.: see General references [e] p. 127.

4.3.6.2 Energetic particles in interplanetary space

4.3.6.2.1 Solar energetic particle composition and charge states

The solar energetic particle events can be separated into two classes, *gradual* and *impulsive* events [99R 01K, 06C], following the classification of flares according to the length of soft X-ray emission [77P]. Energy spectra and elemental abundances as a function of energy are derived from the particle intensities at time of intensity maximum [79V], and from event-integrated flux (or total fluence) measurements [85M].

Large intensity solar energetic particle events (*gradual* events): average abundances from He to Ni can be related to photospheric, solar wind, and coronal abundances [85M]. The abundances are similar to solar wind and coronal abundances [99R], however, with characteristic differences due to mass (M) per charge (Q) dependent fractionation processes [02M]. Compared to photospheric abundances, the abundances from He to Ni are organized by first ionization potential (FIP) [74H, 84F]. Low FIP elements (e.g. Mg, Si, Fe) are overabundant (factor 3 to 5) with respect to local galactic or photospheric abundances [74H, 81M, 85M, 99R]. A discussion of the FIP fractionation mechanism can be found in [98H].

Elemental, isotopic, and ionic charge abundances of elements from H to Ni in solar energetic particle events show large event-to-event variations [71A, 79D, 79M, 99L, 99R, 03L, 06K1] and also large variations within individual events [74V, 76O, 99R, 06K1]. The event-integrated elemental [85B] and isotopic abundances [99L, 03L] are organized by M/Q. After correction for M/Q-dependent fractionation effects they can be used to infer coronal abundances [03L].

Compositional variations before the time of maximum intensity can be attributed to a rigidity dependent scattering mean free path [78S, 81K, 99R, 99T, 00R]; compositional variations before the passage of an interplanetary shock can be understood in terms of models including scattering of heavy ions by proton-amplified waves and a rigidity dependent scattering mean free path [81K, 83L, 99N, 99T, 03N].

^{3}He-rich and heavy ion-rich solar energetic particle events (*impulsive* events): large enhancement of ^{3}He relative to ^{4}He (^{3}He/^{4}He ~0.01 to ≥ 1) [70H, 74B, 75H1, 75H2, 75S]. Abundances of heavy ions increase systematically with mass (or nuclear charge), with enrichment factors of ~10 for Fe at ~1 MeV/nucleon [86M] and ~200 for mass M ~ 200 [00R, 04M]; enrichment factors of heavy ions and ^{3}He are not correlated [77A, 80M, 99R]. Explanation of the overabundance of ^{3}He and heavy ions is given in terms of resonant and non-resonant wave particle interactions [78I, 78F, 83V, 92T, 93M, 98M].

Ionization states: the ionic charge distribution can be determined over a wide energy range from 0.01 to ~ 80 MeV/nucleon (for Fe) by in-situ measurements [76G, 77S, 81H, 84K, 87L, 95M, 95L, 97O, 03L], and by indirect methods, using M/Q-dependent propagation and acceleration characteristics [76O, 99C, 00T, 03D, 03S, 06K2].

There are significant differences of the ionization states of heavy ions in *gradual* and *impulsive* events, in particular for iron. Large (*gradual*) events: below ~10 MeV/nucleon charge states are similar to solar wind charge states (for Fe ~10); at higher energies the mean charge of heavy ions is often increasing with energy [06P]. ^{3}He- and heavy ion-rich events: the ionic charge is strongly energy dependent and increases (for Fe) from ~10-12 at < 0.1 MeV/nucleon to 18-20 at 0.5 MeV/nucleon [03M, 06K3].

The strong energy dependence can be consistently explained by charge stripping during acceleration in the dense environment of the low corona, at altitudes < 0.2 solar radii [00K, 05K, 06D, 07K1, 07K2].

Charge states, in combination with information on energy spectra and intensity-time profiles, can be used to infer acceleration and propagation parameters at the Sun and in interplanetary space [06D, 07K1].

General references for 4.3.6.2.1

a Solar Eruptions and Energetic Particles (Gopalswamy, N., Mewaldt, R.A., Torsti, J., eds.) AGU Geophysical Monograph 165 (2006).
b Coronal Mass Ejections (Kunow, H., Crooker, N.U., Linker, J.A., Schwenn, R., von Steiger, R., eds.) Space Sci Rev. **123** (2006).

Special references for 4.3.6.2.1

70H Hsieh, K.C., Simpson, J.A.: Astrophys. J. **162** (1970) L191.
71A Armstrong, T.P., Krimigis, S.M.: J. Geophys. Res. **76** (1971) 4230.
74B Balasubrahmanyan, V. K. and Serlemitsos, A.T.: Nature **252** (1974) 460.
74H Hovestadt, D.: in Proc. Solar Wind Three (Russell, C.T., ed.), Asilomar (1974) 62.
74V Van Allen, J.A., Venkatarangan, P., Venkatesan, D.: J. Geophys. Res. **79** (1974) 1.
75H1 Hovestadt, D., Klecker, B., Gloeckler, G., et al.: Proc. 14th Int. Cosmic Ray Conf. **5** (1975) 1613.
75H2 Hurford, G.J., Mewaldt, R.A., Stone, E.C., et al.: Astrophys. J. **201** (1975) L95.

75S Serlemitsos, A.T., Balasubrahmanyan, V.K.: Astophys. J. **198** (1975) 195.
76G Gloeckler, G., Sciambi, R.K., Fan, C.Y., Hovestadt, D.: Astrophys. J. **209** (1976) L93.
76O O'Gallagher, J.J., Hovestadt, D., Klecker, B., et al.: Astrophys. J. **209** (1976) L97.
77A Anglin, J.D., Dietrich, W.F., Simpson, J.A.: Proc. 15th Int. Cosmic Ray Conf. **5** (1977) 43.
77P Pallavicini, R., Serio, S., and Vaiana, G.S.: Astrophys. J. **216** (1977) 108.
77S Sciambi, R.K., Gloeckler, G., Fan, C.Y., and Hovestadt, D.: Astrophys. J. **214** (1977) 316.
78F Fisk, L.A.: Astrophys. J. **234** (1978) 1048.
78I Ibragimov, I.A. Kocharov, G.E., Kocharov, L.G.: Dokl. Akad. Nauk SSSR **588** (1978)
78S Scholer, M., Hovestadt, D., Klecker, B., et al.: J. Geophys. Res. **83** (1978) 3349.
79D Dietrich, W.F., Simpson, J.A.: Astrophys. J. **231** (1979) L91.
79M Mewaldt, R.A., Spalding, J.D., Stone, E.C., Vogt, R.E.: Astrophys. J. **231** (1979) L97.
79V Van Hollebeke, M.A.I.: Rev. Geophys. Space Phys. **17** (1979) 545.
80M Mason, G.M., Fisk, L.A., Hovestadt, D., et al.: Astrophys. J. **239** (1980) 1070.
81H Hovestadt, D., Höfner, H., Klecker, B., et al.: Adv. Space Res. **1** (1981) 61.
81K Klecker, B., Scholer, M., Hovestadt, D., et al.: Astrophys. J. **251** (1981) 393.
81M Meyer, J.-P.: Proc. 17th Int. Cosmic Ray Conf. **3** (1981) 145.
83L Lee, M.A.: J. Geophys. Res. **88** (1983) 6109.
83V Varvoglis, H., Papadopoulos, K.: Astrophys. J. **270** (1983) L95.
84F Fan, C.Y., Gloeckler, G., Hovestadt, D.: Space Sci. Rev. **38** (1984) 143.
84K Klecker, B., Hovestadt, D., Scholer, M., et al.: Astrophys. J. **281** (1984) 458.
85B Breneman, H.H., Stone, E.C.: 1985, Astrophys. J. Lett. **299** (1985) L57.
85M Meyer, J.-P.: Astrophys. J. Supp. **57** (1985) 151.
86M Mason, G.M., Reames, D.V., von Rosenvinge, T.T., Klecker, B., Hovestadt, D.: Astrophys. J. **303** (1986) 849.
87L Luhn, A., Klecker, B., Hovestadt, D., Möbius, E.: Astrophys. J. **317** (1987) 951.
92T Temerin, M., Roth, I.: Astrophys. J. **391** (1992) L105.
93M Miller, J.A., Vinas, A.F.: Astrophys. J. **412** (1993) 386.
95L Leske, R.A., Cummings, J.R., Mewaldt, R.A., et al.: Astrophys. J. **452** (1995) L149.
95M Mason, G.M., Mazur, J.E., Looper, M.D., Mewadt, R.A.: Astrophys. J. **452** (1995) 901.
97O Oetliker, M., Klecker, B., Hovestadt, D., Mason, G.M., et al.: Astrophys. J. **477** (1997) 495.
98H Hénoux, J.: Space Sci. Rev. **85** (1998) 215.
98M Miller, J.A.: Space Sci. Rev. **86** (1998) 79.
99C Cohen, C.M.S., Cummings, A.C., Leske, R.A. et al.: Geophys. Res. Lett. **26** (1999) 149.
99L Leske, R.A., Mewaldt, R.A., Cohen, C.M.S., et al.: Geophys. Res. Lett. **26** (1999) 2693.
99N Ng, C.K., Reames, D.V., Tylka, A.T: Geophys. Res. Lett. **26** (1999) 2145.
99R Reames, D.V.: Space Sci. Rev. **90** (1999) 413.
99T Tylka, A.T., Reames, D.V., Ng, C.K.: Geophys. Res. Lett. **26** (1999) 2141.
00K Kocharov, L., Kovaltsov, G.A., Torsti, J., Ostryakov, V.M.: Astron. Astrophys. **357** (2000) 716.
00R Reames, D.V.: Astrophys. J. **540** (2000) L111.
00T Tylka, A.J., Boberg, P.R., McGuire, R.E., et al.: In "Acceleration and Transport of Energetic Particles Observed in the Heliosphere": ACE 2000 Symposium, AIP Vol. **528** (2000) 147.
01K Klein, K.-L., Trottet, G.: Space Sci. Rev. **95** (2001) 215.
02M Mewaldt, R.A., Cohen, C.M.S., Leske, R.A., et al.: Adv. Space Res. **30** (2002) 79.
03D Dietrich, W., and Tylka, A.J.: Proc. 28th Int. Cosmic Ray Conf. **6** (2003) 3291.
03L Leske, R.A., Mewaldt, R.A., Cohen, C.M.S., et al.: Solar Wind Ten, AIP Conf. Proc. **679** (2003), 616.
03M Möbius, E., Cao,Y., Popecki, M.A., et al.: Proc. 28th Int. Cosmic Ray Conf. **6** (2003) 3273.
03N Ng, C.K., Reames, D.V., Tylka, A.J.: Astrophys. J. **591** (2003) 461.
03S Sollitt, L., Stone, E., Mewaldt, R.A., et al.: Proc. 28th Int. Cosmic Ray Conf. **6** (2003) 3295.
04M Mason, G.M, Mazur, J.E., Dwyer, J.R.: Astrophys. J. **606** (2004) 555.
05K Kartavykh, Y.Y., Dröge, W., Kovaltsov, G.A., Ostryakov, V.M.: Solar Phys. **227** (2005) 123.
06C Cane, H.V., Lario, D.: Space Sci. Rev. **123** (2006) 45.
06D Dröge, W., Kartavykh, Y.Y., Klecker, B., Mason, G.M.: Astrophys. J. **645** (2006) 1516.
06K1 Klecker, B., Kunow, H., Cane, H.V., et al.: see General references [b] p. 217.

06K2 Klecker, B., E. Möbius, E., Popecki, M.A.: Space Sci. Rev. **124** (2006) 289.
06K3 Klecker, B., Möbius, E., Popecki, M.A., et al.: Adv. Space Res. **38** (2006) 493.
06P Popecki, M.A.: see General references [a] p. 127.
07K1 Kartavykh, Y.Y., Dröge, W., Klecker, B. , et al.: Astroph. J. **671** (2007) 947.
07K2 Klecker, B., Möbius, E., Popecki, M.A.: Space Sci. Rev. **130** (2007) 273.

4.3.6.2.2 Solar energetic particle injection and coronal propagation

Early observations of non-relativistic [65V, 74L] and relativistic electrons [74S], of protons below ~100 MeV [75V] and at relativistic energies [74P] show a large variability of intensities and intensity-time profiles. These particles originate in solar flare-related acceleration processes or are accelerated by coronal and interplanetary shock waves [99R, 01K, 06C] (see also 4.3.6.2.1).

Particles accelerated in solar flares show velocity dispersion with high energy particles arriving first, low energy particles arriving with a delay that depends on their speed (V), and the distance (S) along the interplanetary magnetic field between the observer and the acceleration site [85R, 99K]. The injection time t_{inj} at the Sun can be inferred for this class of events from the arrival time t_{arr} at the observer by [99K, 06P]

$$t_{arr} = t_{inj} + S/V \quad (1)$$

However, additional delays during interplanetary propagation due to the scattering of the particles [03C], or due to magnetic turbulence related lengthening of the distance S [06R] may also be important. These events are preferentially observed in a range of solar longitudes that are connected to the observer by the interplanetary magnetic field, i.e. at Earth at ~10 - 90° W [88C], suggesting direct access of the accelerated particles to open field lines. Using the inferred injection times, in particular for electrons with small propagation delays, other coronal phenomena (e.g. Radio-, EUV-, X-ray observations) can be related to the particle acceleration [05K]. Injection time profiles of electrons, protons [03D] and heavy ions [06D] have been inferred from a detailed comparison of observed intensity-time and anisotropy-time profiles with interplanetary propagation models.

Particles accelerated at coronal and interplanetary shocks show a large variability of intensity - time profiles, maximum intensity, energy spectra, elemental abundances (see also 4.3.6.2.1) and systematic variations with solar longitude [74R, 75V]. This variability was attributed in the past to a combination of time-extended injection, and coronal and interplanetary propagation [64R, 65A, 74R, 75V, 76N, 76W, 79V]. However, it was shown later that the major controlling agents are the existence of an interplanetary shock, the shock strength and the location of the observer relative to the shock [88C, 06C, 06K]. In these events, the injection can be inferred from a comparison of solar energetic particle measurements with model calculations of shock acceleration [97K, 03N].

References for 4.3.6.2.2

64R Reid, G.C.: J. Geophys. Res. **69** (1964) 2659.
65A Axford, W.I.: Planet. Space Sci. **13** (1965) 1301.
65V Van Allen, J.A., Krimigis, S.M.: J. Geophys. Res. **70** (1965) 5737.
74L Lin, R.P.: Space Sci. Rev. **16** (1974) 189.
74P Pomerantz, M.A., Duggal, S.P.: Rev. Geophys. Space Phys. **12** (1974) 343.
74R Reinhard, R., Wibberenz, G.: Sol. Phys. **36** (1974) 473.
74S Simnett, G.M.: Space Sci. Rev. **16** (1974) 257.
75V Van Hollebeke, M.A.I., MaSung, L.S., McDonald, F.B.: Sol. Phys. **41** (1975) 189.
76N Ng, C.K., Gleeson, L.J.: Sol. Phys. **46** (1976) 347.
76W Wibberenz, G.L., Lanzerotti, J., Venkatesan, D.: J. Geophys. Res. **81** (1976) 5807.
79V Van Hollebeke, M.A.I.: Rev. Geophys. Space Phys. **17** (1979) 545.
85R Reames, D.V., von Rosenvinge, T.T., Lin, R.P.: Astrophys. J. **292** (1985) 716.
88C Cane, H.V., Reames, D.V., von Rosenvinge, T.T.: J. Geophys. Res. **93** (1988) 9555.

97K Kallenrode, M.-B.: J. Geophys. Res. **102** (1997) 22347.
99K Krucker, S., Larson, D.E., Lin, R.P., Thomson, B.J.: Astrophys. J. **519** (1999) 864.
99R Reames, D.V.: Space Sci. Rev. **90** (1999) 413.
01K Klein, K.-L., Trottet, G.: Space Sci. Rev. **95** (2001) 215.
03C Cane, H.V.: Astrophys. J. **598** (2003) 1403.
03D Dröge, W.: Astrophys. J. **589** (2003) 1097.
03N Ng, C.K., Reames, D.V., Tylka, A.J.: Astrophys. J. **591** (2003) 461.
05K Klein, K.-L., Posner, A.: Astron. Astrophys. **431** (2005) 1047.
06C Cane, H.V., Lario, D.: Space Sci. Rev. **123** (2006) 45.
06D Dröge, W., Kartavykh, Y.Y., Klecker, B., Mason, G.M.: Astrophys. J. **645** (2006) 1516.
06K Klecker, B., Kunow, H., Cane, H.V., et al.: Space Sci. Rev. **123** (2006) 217.
06P Posner, A., Klein, K.-L.: Space Sci. Rev. **123** (2006) 238.
06R Ragot, B.R.: Astrophys. J. **653** (2006) 1493.

4.3.6.2.3 Interplanetary propagation of solar cosmic rays

Energetic particles accelerated in flares at the Sun or by coronal and interplanetary shocks are scattered by magnetic irregularities in the solar wind. Their propagation in the corona and in interplanetary space can be described by the combined effects of pitch angle scattering, convection, adiabatic energy loss in the expanding solar wind, and the focussing effect of the diverging magnetic field [a, b, c, 65P]. Depending on the level and nature of magnetic field turbulence, the propagation can be described as a diffusive process, or as an almost scatter-free process [65P, 75N, 76E1,76E2, 90D, 91K].

The diffusion coefficient and the scattering mean free path λ are derived from the measurements of protons [77H, 77W, 78M] and electrons [92K, 94B]. A compilation of mean free path at different rigidities can be found in [77Z, 78Z]. Typical values of λ parallel to the magnetic field of a 10 MeV proton at 1 AU solar distance, in large solar energetic particle events, is ~ 0.05 - 0.2 AU. However, for low turbulence levels, it can be as large as ~1 AU (scatter free propagation).

Literature for:
Scatter-free propagation of protons [75P, 77W] and electrons [74L].
Anisotropies and scattering parameters [71M, 73I]
Radial dependence of scattering mean free path λ [77H, 77W].

Scattering theory: Scattering parameters can be derived from the turbulence level of the interplanetary magnetic field [66J, 68H]. The application of quasi-linear theory (QLT) and the assumption of slab (1D) turbulence results in a scattering mean free path that is significantly smaller than derived from particle intensity-time profiles and anisotropy measurements [82P]. This discrepancy can be solved by an extension of QLT including dynamical and dissipative effects [94B] and by assuming a mixture of ~20% slab (1D) and ~80% 2D turbulence [94B, 00D].

ESP events: Energetic storm particle (ESP) events are long lasting (~ hours) intensity enhancement of ~MeV ions, related to the passage of an interplanetary shock [65B, 67M, 67R]. Typical signatures are: exponential decrease of particle intensity with distance from the shock [81K]; rigidity-dependent e-folding distance [81K]; variation of elemental abundances of particles of the same velocity but different rigidity during ESP event [69L, 72S, 81K]. Explanation in terms of shock acceleration of solar wind or suprathermal particles from previous events [71F, 75S, 99M, 03N]. The acceleration of suprathermal particles from previous events is consistent with the finding of a moderate enhancement of ^{3}He and heavy ions in many shock-related events [99C, 99M, 01D]. ESP events at high latitudes are described in [04L1], the statistics of ESP events in [04L2].
Shock-spike events: short-lived intensity enhancements (~ 10 min) at MeV energies, associated with the passage of an interplanetary shock are described in [71O, 71P, 71S, 77A1]. An explanation in terms of acceleration at quasi-perpendicular shocks is found in [77A1, 83D, 90D].

The theory of particle acceleration at parallel and perpendicular shocks can be studied in [77A2, 78B, 83L]; the simulation of shock acceleration, including propagation is described in [75S, 97K, 03N].

References for 4.3.6.2.3

General references

a Interplanetary Dynamical Processes (Parker, E.N., ed.), Wiley-Interscience London (1963).
b Study of Travelling Interplanetary Phenomena (Shea, M.A., Smart, D.F., Wu, S.T., eds.), Astrophys. Spac Sci. Library 71, Reidel Publ. Comp. Dordrecht (1977).
c Physics of the Inner Heliosphere, II. Particles, Waves, and Turbulence (Schwenn, R., Marsch, E., eds.), Berlin, Springer Verlag (1991).

Special references

65B Bryant, D.A., Cline, T.L., Desai, U.D., McDonald, F.B.: Astrophys. J. **141** (1965) 478.
65P Parker, E.N.: Planet. Space Sci. **13** (1965) 9.
66J Jokipii, J.R.: Astrophys. J. **146** (1966) 480.
67M McCracken, K.G., Rao, U.R., Bukata, R.P.: J. Geophys. Res. **72** (1967) 4293.
67R Rao, U.R., McCracken, K.G., Bukata, R.P.: J. Geophys. Res. **72** (1967) 4325.
68H Hasselmann, K., Wibberenz, G.: Zeitschrift Geophys. **34** (1968) 353.
69L Lanzerotti, L.J., Robbins, M.F.: Sol. Phys. **10** (1969) 212.
71F Fisk, L.A.: J. Geophys. Res. **76** (1971) 1662.
71M McCracken, K.G., Rao, U.R., Bukata, R.P., Keith, E.P.: Sol. Phys. **18** (1971) 100.
71O Ogilvie, K.W., Arens, J.F.: J. Geophys. Res. **76** (1971) 13.
71P Palmeira, R.A.R., Allum, F.R., Rao, U.R.: Sol. Phys. **21** (1971) 204.
71S Singer, S., Montgomery, M.D.: J. Geophys. Res. **76** (1971) 6628.
72S Scholer, M., Hovestaft, D., Häusler, B.: Sol. Phys. **24** (1972) 475.
73I Innanen, W.G., Van Allen, J.A.: J. Geophys. Res. **78** (1973) 1019.
74L Lin, R.P.: Space Sci. Rev. **16** (1974) 189.
75N Nolte, J.T., Roelof, E.C.: Proc. 14th Int. Cosmic Ray Conf. **5** (1975) 1019.
75P Palmer, I.D., Palmeira, R.A.R., Allum, F.R.: Sol. Phys. **40** (1975) 449.
75S Scholer, M., Morfill, G.: Sol. Phys. **45** (1975) 227.
76E1 Earl, J.S.: Astrophys. J. **205** (1976) 900.
76E2 Earl, J.S.: Astrophys. J. **206** (1976) 301.
77A1 Armstrong, T.P., Chen, G., Sarris, E.T., Krimigis, S.M.: see General references [b], p. 367.
77A2 Axford, W. I., Leer, E., and Skadron, G.: Proc. 15th Int. Cosmic Ray Conf. **11** (1977) 132.
77H Hamilton, D.C.: J. Geophys. Res. **82** (1977) 2157.
77W Wibberenz, G.: see General references [b] 323.
77Z Zwickl, R.D., Webber, W.R.: Sol. Phys. **54** (1977) 457.
78B Blandford, R.D., Ostriker, J.P.: Astrophys. J. Lett. **221** (1978) L29.
78M MaSung, L.S., Earl, J.A.: Astrophys. J. **222** (1978) 1080.
78Z Zwickl, R.D., Webber, W.R.: J. Geophys. Res. **83** (1978) 1157.
81K Klecker, B., Scholer, M., Hovestadt, D., Gloeckler, G., Ipavich, F.M.: Astrophys. J. **251** (1981) 393.
82P Palmer, I.D.: Rev. Geophys. **20** (1982) 335.
83D Decker, R.B.: J. Geophys. Res. **88** (1983) 9959.
83L Lee, M.A.: J. Geophys. Res. **88** (1983) 6109.
90D Decker, R.B.: J. Geophys. Res. **95** (1990) 11993.
91K Kunow, H., Wibberenz, G., Green, G., et al.: see General references [c] p. 243.
92K Kallenrode, M.-B., Wibberenz, G., Hucke, S.: Astrophys. J. **394** (1992) 351.
94B Bieber, J.W., Matthaeus, W.H., Smith, C.W., et al.: Astrophys. J. **420** (1994) 294.
97K Kallenrode, M.-B., Wibberenz, G.: J. Geophys. Res. **102** (1997) 22311.
99C Cohen, C.M.S., Cummings, A.C., Leske, R.A., et al.: Geophys. Res. Lett. **26** (1999) 149.

99M Mason, G.M., Mazur, J.E., Dwyer, J.R.: Astrophys. J. Lett. **525** (1999) L133.
00D Dröge, W.: Space Sci. Rev. **93** (2000) 121.
01D Desai, M.I., Mason, G.M., Dwyer, J.R., et al.: Astrophys. J. Lett. **553** (2001) L89.
03N Ng, C.K., Reames, D.V., Tylka, A.J.: Astrophys. J. **591** (2003) 461.
04L1 Lario, D., Decker, R.B., Roelof, E.C., et al.: J. Geophys. Res. **109** (2004) A01107.
04L2 Lario, D., Hu, Q., Ho, G.C., et al: Proc. Solar Wind 11 – SOHO 16, ESA SP-592 (2005).

4.3.6.2.4 Corotating energetic particle events

Long-lived streams of low energy (~0.01 - 10 MeV/nucleon) ions and ~40 - 300 keV electrons near corotating interaction regions (CIR) resulting from the interaction of high-speed solar wind overtaking slow-speed solar wind and forming forward and reverse waves. If the waves are sufficiently strong, a shock pair is formed, with the forward shock (FS) propagating outward and the reverse shock (RS) propagating inward [76B, 76M, 78P1, 80S, 81C, 98K, 98S].

Duration of CIRs is ~ 4 - 10 days, flux of 1 MeV protons at 1 AU is ~10-100 (p/cm^2 s sr MeV) [98S].

Peak intensity at ~4 AU is given in [78V, 99M]; heliocentric gradient between 0.3 and 1 AU: ~ 350% per AU [77K, 78V], between 1 AU and 4 AU: ~ 100% per AU [78V], and between 4 AU and 9 AU: variable from –40% per AU to –100% per AU [78V].

Energy spectra of ions: in the energy range of ~0.15 to ~10 MeV/nucleon the energy spectra can be described by a distribution function with an exponential dependence on speed [79G], by differential energy spectra with an exponential dependence on momentum [99M], or by a power law in energy per nucleon with a break (steepening) at > 1 MeV/nucleon [97M].

Elemental composition (H - Fe) at 1 AU is similar to the composition in the solar wind and in large (gradual) solar energetic particle events [78G, 79S, 93R, 98K, 99M , 99R].

The average ionic charge of C, O, Mg, and Fe at 1 AU is similar to the average ionic charge of the solar wind, suggesting a solar wind source [02M1, 02M2]. Helium shows at 1 AU ~10% to ~60% pickup He^+ (relative to He^{2+}) of interstellar origin [00C, 03K], that increases with increasing distance from the Sun, with He^+ dominating at 4.5 AU [94G].

Ion anisotropies in CIRs [97D1]

Electron observations: at mid latitudes [95S], and at high latitudes [96R].

Model of corotating streams [78P2, 99G2], acceleration models [80F, 96S, 99S], comparison of ion data with model predictions [96S, 97R, 99M], acceleration efficiency in CIRs [97D2].
CIRs in the inner heliosphere [99B], in the outer heliosphere [99L], and at high latitudes [99G1, 99K].

Special References for 4.3.6.2.4

76B Barnes, C.W., Simpson, J.A.: Astrophys. J. **210** (1976) L91.
76M McDonald, F.B., Teegarden, B.J., Trainor, J.H., et al.: Astrophs. J. **203** (1976) L149.
77K Kunov, H., Wibberenz, G., Green, G., et al.: Proc. 15th Int. Cosmic Ray Conf. **3** (1977) 227.
78G McGuire, R.E., von Rosenvinge, T.T., McDonald, F.B.: Astrophs. J. **224** (1978) L87.
78P1 Pesses, M.E., van Allen, J.A., Goertz, C.A.: J. Geophys. Res. **83** (1978) 553.
78P2 Pizzo, V.: J. Geophys. Res. **83** (1978) 5563.
78V Van Hollebeke, M.A.I., McDonald, F.B., Trainor, J.H., et al.: J. Geophys. Res. **83** (1978) 4723.
79G Gloeckler, G., Hovestadt, D., Fisk, L.A.: Astrophys. J. **230** (1979) L191.
79S Scholer, M., Hovestadt, D., Klecker, B., Gloeckler, G.: Astrophys. J. 227 (1979) 323.
80F Fisk, L.A., Lee, M.A.: Astrophys. J. **237** (1980) 620.
80S Scholer, M., Morfill, G., van Hollebeke, M.A.I.: J. Geophys. Res. **85** (1980) 1743.
81C Christon, S.P.: J. Geophys. Res. **86** (1981) 8852.
93R Richardson, I.G., Barbier, L.M., Reames, D.V., et al.: J. Geophys. Res. **98** (1993) 13.
94G Gloeckler, G., Geiss, J., Roelof, E.C., et al.: J. Geophys. Res. **99** (1994) 17637.
95S Simnett, G.M., Roelof, E.C.: Space Sci. Rev. **72** (1995) 303.
96R Roelof, E.C., Simnett, G.M., Tappin, S.J.: Astron. Astrophys. **316** (1996) 481.
96S Schwadron, N.A., Fisk, L.A., Gloeckler, G.: Geophys. Res. Lett. **23 (21)** (1996) 2871.

97D1 Dwyer, J.R., Mason, G.M., Mazur, J.E., et al.: Astrophys. J. **490** (1997) L115.
97D2 Desai, M.I., Marsden, R.G., Sanderson, T.R., et al.: Geophys. Res. Lett. **24** (1997) 1155.
97M Mason, G.M., Mazur, J.E., Dwyer, J.R.: Astrophys. J. **486** (1997) L149.
97R Reames, D.V., Ng, C.K., Mason, G.M., Dwyer, J.R., Mazur, J.E., von Rosenvinge, T.T.: Geophys. Res. Lett. **24** (1997) 2917.
98K Keppler, E.: Surveys Geophys **19** (1998) 211.
98S Simnett, G.M., Kunow, H., Flückiger, E., et al.: Space Sci. Rev. **83** (1998) 215.
99B Balogh, A., Bothmer, V., Crooker, N.U., et al.: Space Sci. Rev. **89** (1999) 135.
99G1 Gazis, P.R., McDonald, F.B., Burger, R.A., et al.: Space Sci. Rev. **89** (1999) 269.
99G2 Gosling, J.T., Pizzo, V.J.: Space Sci. Rev. **89** (1999) 21.
99K Kunow, H., Lee, M.A., Fisk, L.A., et al.: Space Sci. Rev. **89** (1999) 221.
99L Lazarus, A.J., Richardson, J.D., Decker, R.B., McDonald, F.B.: Space Sci. Rev. **89** (1999) 53.
99M Mason, G.M., von Steiger, R., Decker, R.B., et al.: Space Sci. Rev. **89** (1999) 301.
99R Reames, D. V.: Space Sci. Rev. **90** (1999) 413.
99S Scholer, M., Mann, G., Chalov, S., et al.: Space Sci. Rev. **89** (1999) 369.
00C Chotoo, K., Schwadron, N.A., Mason, G.M., et al.: J. Geophys. Res. **105(14)** (2000) 23107.
02M1 Mazur, J.E., Mason, G.M., and Mewaldt, R.A.: Astrophys. J. **566** (2002) 555.
02M2 Möbius, E., Morris, D., Popecki, M.A., Klecker, B., Kistler, L.M., Galvin, A.B.: Geophys. Res. Lett. **29** (2002) doi: 10.1029/2001GL013410.
03K Kucharek, H., Möbius, E., Li, W., Farrugia, C.J., et al.: J Geophys. Res. **108** (2003) 8040.

4.3.6.2.5 Modulation of galactic cosmic rays

Galactic cosmic rays are observed in the heliosphere with energies in the range of ~1 to 1015 MeV [01S]. Below ~104 MeV the galactic cosmic rays are considerably modulated: Their propagation from interstellar space through the heliosheath into the inner Solar System can be described by the combined effects of diffusion, convection, energy loss by adiabatic deceleration and drift [65P, 77J, 98P]. Because drift effects depend on the direction of the magnetic field and the charge of the particles [77J], the modulation shows the 22 year cycle of the solar large scale magnetic field, and characteristic differences for electrons and ions [98E]. While galactic cosmic rays diffuse inwards they are continuously convected out by the solar wind and loose energy in the radially expanding solar wind. This leads to a decrease of the intensity of the modulated H, He and heavy ion spectra with energy at energies less than a few hundred MeV/nucleon (Fig. 2) with the spectral shape becoming insensitive to the shape of the interstellar spectra [65P, 75V]. Furthermore, galactic cosmic rays are modulated by the passage of large-scale interplanetary disturbances propagating into the outer heliosphere [93M, 98W]. A significant fraction of the total modulation occurs in the heliosheath [00M, 02M].

Elemental and isotopic composition of galactic cosmic rays: [83M]; age of galactic cosmic rays as derived from radioactive "clocks": [01M]; origin of galactic cosmic rays: [07W].

The solar cycle variation of galactic cosmic rays is observed by ground based neutron monitor stations and experiments in space [58F, 74P, 76M]. The annual mean nucleonic intensity at neutron monitor energies is inversely correlated with the sunspot number R_Z [58F, 00V]. The solar cycle variation depends on energy and is about a factor of 2 for protons with $E > 80$ MeV in interplanetary space and ~18 % at 2.2 GeV, respectively [00V]. There is a time lag of ~1 year between cosmic ray intensity peak and sunspot minimum [01S]. This time lag can be interpreted in terms of diffusion and convection of galactic cosmic rays. In the limit of small and large diffusion coefficients κ, the time lag is given by R_B/V_{SW} and R_B^2/κ, respectively, where R_B and V_{SW} are the distance to the modulating boundary and the solar wind convection speed, respectively [75O].

Hysteresis effects in the modulation are described in [72V, 72S, 73B].

Galactic cosmic ray electron spectrum and change with time: [71M, 98E].

Anisotropies: Interpretation of north-south anisotropy of ~0.2% at neutron monitor energies as being due to radial gradient: [71B, 72I, 72O]. Measurements of the azimuthal anisotropy at > 480 MeV/nucleon for H, He up to 3 AU: [75A]. Azimuthal anisotropy in the ecliptic plane leads to diurnal cosmic ray variations. At neutron monitor energies the long-term average amplitude of anisotropy is ~0.4% [71R, 72O, 73F]. An explanation in terms of corotation anisotropy is given in [71P].

Radial and latitudinal gradients in the heliosphere: Direct measurements of integral gradients as a function of radial distance and latitude have been obtained with Pioneer 10, 11, Voyager 1, 2, and Ulysses; baseline measurements at 1AU have been obtained with IMP-6/7/8, ISEE-1/3, SOHO and ACE. Gradient measurements of galactic cosmic ray protons and helium are presented in [73M, 77M1, 77M2, 82M, 85M, 97F, 97M, 99W], and of electrons in [98E]. The radial and latitudinal gradients depend on many parameters, including the phase of the solar cycle, particle rigidity, and distance from the Sun. The radial gradient g_r can be described as $g_r = G_0\, r^{\alpha}$ [97F]. Table 1 shows typical values of G_0 and α for solar minimum (1977, 1987) and solar maximum conditions (1981, 1990), derived for heliocentric distances between 1 and 66 AU [97F]. The latitudinal gradients depend on the direction of the large scale interplanetary magnetic field and are generally small [89M, 97M], for example ~1.2±0.1%/degree and –1.6±0.3%/degree for 29-67 MeV/nucleon He in 1975-1976 and 1985-1986, respectively [89M].

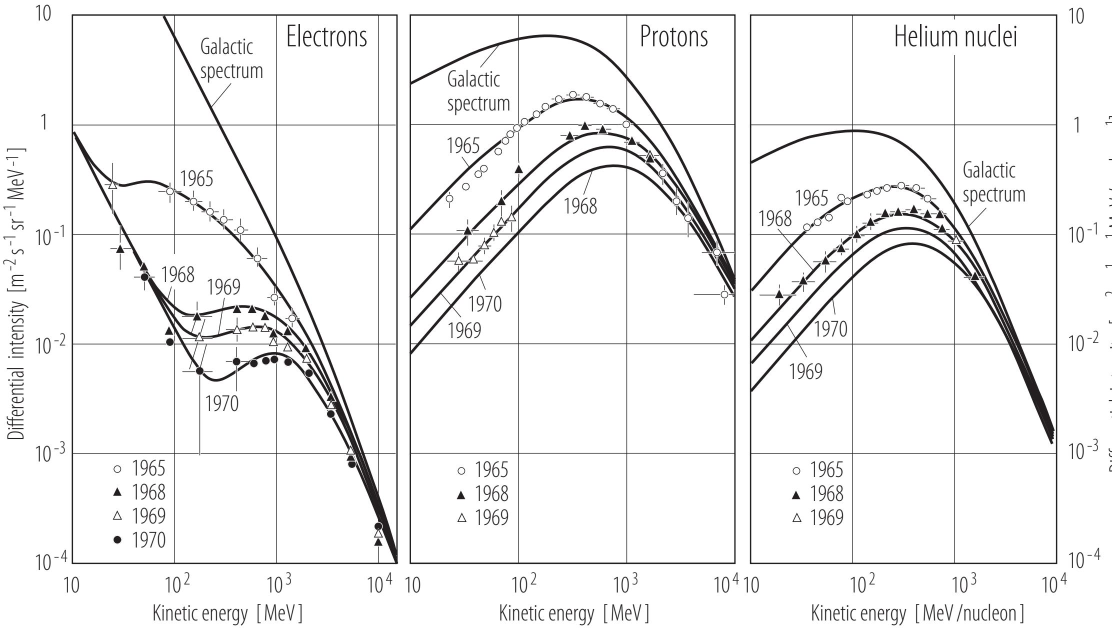

Fig. 2. Observed and calculated proton, helium, and electron spectra at 1 AU for 1965, 1968, 1969 and 1970 [72U].

Forbush decrease: Forbush decreases are large, sudden, asymmetrical depressions in the cosmic ray flux, lasting several days. The decrease phase is ~12 to 24 hours long, recovery takes at 1 AU typically several days [71L, 86L]. The decrease is correlated with large scale disturbances in the solar wind, i.e. with coronal mass ejections , interplanetary shocks [96C, 00C], and corotating interaction regions [98S]. The maximum reduction of cosmic ray intensity as observed by the worldwide neutron monitor stations is ~3-20%, depending on energy (or latitude) [98W]. The intensity decrease and recovery can be modelled in terms of outward propagating diffusive barriers with different propagation characteristics [91L, 98W].

Table 1. Radial gradients of galactic cosmic rays for solar minimum and solar maximum conditions [97F]

	Solar minimum		Solar maximum	
	1977	1987	1981	1990
H 130-225 MeV/nuc				
α	−0.7±0.05	−0.3±0.02	0.7±0.1	0.27±0.1
G_0 [%/AU]	13±1.5	5.5±0.5	0.6±0.2	1.00±0.3
He 180-450 MeV/nuc				
α	−1.1±1	−0.74±0.04	−0.11±0.05	−0.3±0.1
G_0 [%/AU]	17.4±0.04	0.12±0.02	0.5±0.6	6.5±2

References for 4.3.6.2.5

58F Forbush, S.E.: J. Geophys. Res. **63** (1958) 651.
65P Parker, E.N.: Planet. Space Sci. **13** (1965) 9.
71B Bercovich, M.: Proc. 12th Intern. Cosmic Ray Conf. **2** (1971) 579.
71L Lockwood, J.A.: Space Sci. Rev. **12** (1971) 658.
71M Meyer, P., Schmidt, P.J., L'Heureux, J.: Proc. 12th Intern. Cosmic Ray Conf. **2** (1971) 548.
71P Pomerantz, M.A., Duggal, S.P.: Space Sci. Rev. **12** (1971) 75.
71R Rao, U.R.: Space Sci. Rev. **12** (1971) 719.
72I Iucci, N., Storini, M.: Nuovo Cimento **10** (1972) 325.
72O O'Gallagher, J.J.: Rev. Geophys. Space Phys. **10** (1972) 821.
72S Schmidt, P.J.: J. Geophys. Res. **77** (1972) 3295.
72U Urch, I.H., Gleeson, L.J.: Astrophys. Space Sci. **17** (1972) 426.
72V Van Hollebeke, M.A.I., Wang, J.R., McDonald, F.B.: J. Geophys. Res. **77** (1972) 6881.
73B Burger, J.J., Swanenburg, B.N.: J. Geophys. Res. **78** (1973) 292.
73F Forbush, S.E.: J. Geophys. Res. **78** (1973) 7933.
73M McKibben, R.B., O'Gallagher, J.J., Simpson, J.A., et al.: Astrophys. J. **181** (1973) L9.
74P Pomerantz, M.A., Duggal, S.P.: Rev. Geophys. Space Phys. **12** (1974) 343.
75A Axford, W. I., Fillius, W., Gleeson, L.J., Mogro-Campero, A.: Proc. 14th Int. Cosmic Ray Conf. **4** (1975) 1519.
75O O'Gallagher, J.J.: Astrophys. J. **197** (1975) 495.
75V Völk, H.J.: Rev. Geophys. Space Phys. **13** (1975) 547.
76M Moraal, H.: Space Sci. Rev. **19** (1976) 845.
77J Jokipii, J.R., Levy, E. H., Hubbard, W. B.: Astrophys. J. **213** (1977) 861.
77M1 McDonald, F.B., Lal, N., Trainor, J.H., et al.: Astrophys. J. **216** (1977) 930.
77M2 McKibben, R.B., O'Gallagher, J.J., Pyle, K.R., Simpson, J.A.: Proc. 15th Int. Cosmic Ray Conf. **3** (1977), 240.
82M McKibben, R.B., Pyle, K.R., Simpson, J.A.: Astrophys. J. **254** (1982) L23.
83M Mewaldt., R.A.: Rev. Geophys. Space Phys. **21** (1983) 295.
85M McKibben, R.B., Pyle, K.R., Simpson, J.A.: Astrophys. J. **289** (1985) L35.
86L Lockwood, J.S., Webber, W.R., Jokipii, J.R.: J. Geophys. Res. **91** (1986) 2851.
89M McKibben, R.B.: J. Geophys. Res. **94** (1989) 17021.
91L LeRoux, J.A., Potgieter, M.S.: Astron. Astrophys. **243** (1991) 531.
93M McDonald, F.B., Lal, N., McGuire, R.E.: J. Geophys. Res. **98** (1993) 1243.
96C Cane, H.V., Richardson, I.G., von Rosenvinge, T.T.: J. Geophys. Res. **101** (1996) 21561.
97F Fujii, Z., McDonald, F.B.: J. Geophys. Res. **102** (1997) 24201.
97M McDonald, F.B., Ferrando, P., Heber, B., et al.: J. Geophys. Res. **102** (1997) 4643.
98E Evenson, P.: Space Science Rev. **83** (1998) 63.
98P Potgieter, M.S.: Space Science Rev. **83** (1998) 147.
98S Simpson, J.A.: Space Science Rev. **83** (1998) 169.

98W Wibberenz, G., le Roux, J.A., Potgieter, M.S., Bieber, J.W.: Space Sci. Rev. **83** (1998) 309.
99W Webber, W.R., Lockwood, J.A.: J. Geophys. Res. **104** (1999) 2487.
00C Cane, H.V.: Space Sci. Rev. **93** (2000) 55.
00M McDonald, F.B., Heikkila, B., Lal, N., Stone, E.C.: J. Geophys. Res. **105** (2000) 1.
00V Van Allen, J.: Geophys. Res. Lett. **27** (2000) 2453.
01M Mewaldt, R.A., Yanasak, N.E., Wiedenbeck, M.E., et al.: Space Sci. Rev. **99** (2001) 27.
01S Swordy, S.P.: Space Sci. Rev. **99** (2001) 85.
02M McDonald, F.B., Klecker, B., McGuire, R.E., Reames, D.V.: J. Geophys. Res. **107** (2002) SSH 2-1.
07W Wiedenbeck, M.E., Binns, W.R., Cummings, A.C., et al.: Space Sci. Rev. **130** (2007) 415.

4.3.6.2.6 Anomalous component of low energy cosmic rays

The anomalous component of low energy cosmic rays (ACR) has been discovered in 1975 in the inner heliosphere. The 'anomalous' feature was the flat energy spectrum of ^{4}He between 10 and 80 MeV/nucleon, and the "hump" (Fig. 3) in the quiet-time cosmic ray energy spectrum of heavy ions (predominantly N, O, and Ne) at energies of ~3-20 MeV/nucleon, with unusual composition (C/O < 0.1). The early measurements showed He [73G], O [73H, 74M], N [74M] and Ne [75V, 77K] in anomalous cosmic rays. Later, in the outer Solar System, also Ar [87C], and H [88C, 89S, 95C1, 95M] was identified in ACRs. The measurements of relative abundances of elements with nuclear charge $1 \leq Z \leq 26$ are summarized in Table 1. The early measurements also showed a positive radial gradient and modulation similar to galactic cosmic rays, suggesting a source in the outer Solar System [74F, 74M, 75M, 76F].

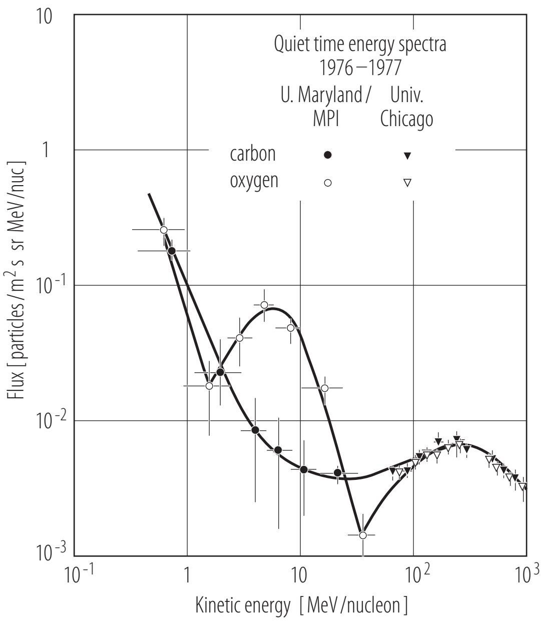

Fig. 3. Spectra of quiet time C and O. The anomalous feature is the "hump" at energies of 3 to 20 MeV/nucleon with a C/O ration < 0.1, different from the composition of solar and galactic cosmic rays [73H, 74M].

Radial and latitudinal gradients: Radial and latitudinal gradients were derived from measurements with many spacecraft in the inner (IMP, SAMPEX) and outer heliosphere (Pioneer 10/11, Voyager 1/2, Ulysses). Similar to GCRs (see 4.3.6.2.5), the radial and latitudinal gradients depend on particle rigidity, location in the heliosphere and phase of the solar cycle [87C, 89M, 95C2, 96T, 98M, 99F]. Typical large-scale radial gradients of ACR oxygen at 7-25 MeV/nucleon between 1 AU and 41 AU (1987) and between 1 and 58 AU (1993) are 8.8±0.6 %/AU and 2.2±0.8%/AU, respectively [95C2]. A characteristic feature consistently observed in several solar cycles is the sign change of the latitude gradient in consecutive solar cycles (see Table 2), simultaneously with the change in direction of the large scale solar magnetic field, implying the importance of drift effects for ACR propagation.

Because all elements initially identified as ACRs had high first ionization potential (He, N, O, Ne), interstellar neutral particles were suggested as a source, that are singly ionized in the inner Solar System, picked up by the solar wind, convected with the solar wind into the outer heliosphere, and accelerated in the outer heliosphere [74F] and at the termination shock [81P].

ACR Models: A comparison with detailed numerical models, including acceleration at the termination shock, convection, radial diffusion, and gradient and curvature drift effects showed that the hypothesis of an interstellar origin was basically correct [81P, 86J, 88P, 98J]. It was found that taking the drift effects into account is essential for explaining the different radial and latitudinal gradients in subsequent solar cycles with different polarity of the heliospheric magnetic field [86J, 98S]. The models assuming acceleration at the termination shock (TS) predicted the unfolding of the ACR energy spectra into single power law spectra, characteristic for local shock acceleration. However, the measurements of the Voyager 1 spacecraft that encountered the TS in 2004 [05S] continued to show the modulation of ACRs. Possible explanations are that the acceleration at the termination shock is not locally, where the Voyager 1 crossed the TS, but, due to its blunt, non-spherical structure, on the flanks [07J, 07S], or that the acceleration is at larger distances, i.e. in the distant heliosheath [07S].

Table 1. Relative abundances of ACRs, normalized to oxygen [98K, 99R, 02C], compared with Solar System abundances [07G] and the abundances of galactic cosmic rays as measured near Earth [90E].

Ion	Anomalous cosmic rays: Interplanetary 5 [MeV/nuc] [1]	Spectral Fit [2]	Filtration (Q=1) 8-20 [MeV/nuc] [3]	Solar System [07G]	Galactic [90E]
He	500 ± 50	970 ± 50		18621	
C	< 1	0.49 ± 0.05	0.9 ± 0.5	53.7	109
N	12 ± 1	14 ± 0.8		13.2	32
O	100	100	70	100	100
Ne	7 ± 0.7	6.5 ± 0.4	3.5 ± 0.3	15.1	16.76
Mg	0.12 ± 0.03	0.037 ± 0.013	0.07 ± 0.03	7.41	20.67
Si	0.17 ± 0.03	0.12 ± 0.02	< 0.03	7.08	15.85
S	0.06 ± 0.02	0.039 ± 0.013	< 0.03	3.02	3.46
Ar	0.42 ± 0.05	0.50 ± 0.09	< 0.02	0.33	1.48
Fe	< 0.09		< 0.02	6.17	9.51
Kr	< 0.002				

[1]Derived from measurements at 1 AU [99R]; [2]Derived from Voyager measurements in the outer heliosphere [02C]; [3]Using ionic charge information derived from the rigidity dependent cutoff of particles in the magnetic field of the Earth [98K].

Table 2. Typical latitudinal gradients of ACRs in three solar cycles

	1975-1976			1987			1992-1995		
Ion	Energy [MeV/n]	Lat. gradient [%/°]	Ref.	Energy [MeV/n]	Lat. gradient [%/°]	Ref.	Energy [MeV/n]	Lat. gradient [%/°]	Ref.
He	11-20	1.5±0.2	89M	20 - 25	–4.3	90C1	10 - 22	2.1 ± 0.16	99F
O				7 - 25	–5.6	90C1	10	1.3 ± 0.4	95C2
Ne							9 - 30	2.0 ± 0.4	96T

Ionization state of ACRs: the hypothesis of an interstellar source implied that ACRs should be singly ionized [74F]. Ionization states, indirectly inferred from (1) modulation effects in the heliosphere [77M, 80K, 88M], and (2) propagation in the Earth's magnetic field [89O, 90B, 91S] provided upper limits: the ionic charge Q of ACR oxygen and neon was found to be consistent with $Q \leq 2$ [89O, 90B] and $Q = 1$ [91S], respectively. A comparison of interplanetary with magnetospheric oxygen intensities at 5 to 20

MeV/nucleon showed $Q = 1$ for oxygen [91A]. Conclusive evidence came from the direct measurement of the ionic charge of N, O, and Ne for a large number of ions, using the cutoff of the Earth's magnetic field: It was found that $Q = 1$ for N, O, and Ne at 8 to 16 MeV/nucleon [95K], and that N, O, and Ne are multiply charged at higher energies [96M, 98K]. The higher charge states at higher energies are consistent with charge exchange during acceleration in the outer heliosphere [96J].

ACRs in the magnetosphere: singly charged anomalous cosmic rays have access to the inner magnetosphere and, after charge exchange at low altitudes, can be trapped, resulting in stably trapped particles (predominantly N, O, Ne) in the magnetosphere [91G, 93C, 95S].

ACRs of non-interstellar origin: The comparison of high-sensitivity measurements in the outer heliosphere with modulation calculations showed that there is also a small (a few per cent compared to Solar System abundances, see Table 1) singly ionized heliospheric component, such as Na, Mg, Si, and S [07C]. The abundances of these ions cannot be accounted for by the local interstellar medium [02S2, 07C]. A possible source are sputtered atoms from small grains in the Kuiper asteroid belt at some 30-50 AU from the sun, subsequently ionized and picked up in the solar wind [02S1].

Isotopic composition: predominantly ^{4}He, ^{14}N, ^{16}O, with small abundances of ^{18}O (^{18}O/^{16}O ~0.002), and ^{22}Ne (^{22}Ne/^{20}Ne ~ 0.1) [76M, 96L, 99L].

Composition of the local interstellar medium: With interstellar neutrals being the dominant source of ACRs, the composition of the local interstellar medium can be derived from the anomalous cosmic ray composition [90C2]. This method is particularly of interest for elements like Ar [02C] where pickup ion measurements are not available (see also 4.3.6.3.2).

References for 4.3.6.2.6

Special References

73G Garcia-Munoz, M., Mason, G.M., Simpson, J.A.: Astrophys. J. **182** (1973) L81.
73H Hovestadt, D., Vollmer, O., Gloeckler, G., Fan, C.Y.: Phys. Rev. Lett. **31** (1973) 650.
74F Fisk, L.A., Kozlovsky, B., Ramaty, R.: Astrophys. J. **190** (1974) L35.
74M McDonald, F.B., Teegarden, B.J., Trainor, J.H., Webber, W.R.: Astrophys. J. **187** (1974) L105.
75M McKibben, R.B., Pyle, K.R., Simpson, J.A., et al.: Proc. 14th Int. Conf. Cosmic Rays, **4** (1975) 1512.
75V Von Rosenvinge, T.T., McDonald, F.B.: Proc. 14th Int. Conf. Cosmic Rays, **2** (1975) 792.
76F Fisk, L.A.: Astrophys. J. **206** (1976) 333.
76M Mewaldt, R.A., Stone, E.C., Vidor, S.B., Vogt, R.R.: Astrophys. J. **205** (1976) 931.
77K Klecker, B., Hovestadt, D., Gloeckler, G., Fan, C.Y.: Astrophys. J. **212** (1977) 290.
77M McKibben, R.B.: Astrophys. J. **217** (1977) L113.
80K Klecker, B., Hovestadt, D., Gloeckler, G., Fan, C.Y.: Geophys. Res. Lett. **7** (1980) 1033.
81P Pesses, M.E., Jokipii, J.R., Eichler, D.: Astrophys. J. **246** (1981) L85.
86J Jokipii, J.R.: J. Geophys. Res. **91** (1986) 2929.
87C Cummings, A.C, Stone, E.C.: Proc. 20th Intern. Cosmic Ray Conf. **4** (1987) 180.
88C Christian, E.R., Cummings, A.C., Stone, E.C.: Astrophys. J. **334** (1988) L77.
88M McDonald, F.B., Lal, N., Perko, J.S., von Rosenvinge, T.T.: Astrophys. J. **333** (1988) L109.
88P Potgieter, M.S., Moraal, H.: Astrophys. J. **330** (1988) 445.
89M McKibben, R.B.: J. Geophys. Res. **94** (1989) 17021.
89O Oschliess, K. Beaujjean, R., Enge, W.: Astrophys. J. **345** (1989) 776.
89S Stone, E.C.: Adv. Space Res. **9** (1989) 15.
90B Biswas, S., Durgaprasad, N, Mitra, B., Singh, R.K.: Astrophys. J. **359** (1990) L5.
90C1 Cummings, C.A., Mewaldt, R.A., Stone, E.C., Webber, W.R.: Proc. 21st Int. Cosmic Ray Conf. **6** (1990) 206.
90C2 Cummings, C.A., Stone, E.C.: Proc. 21th Int. Cosmic Ray Conf. **6** (1990) 202.
90E Engelmann, J.J., Ferrando, P., Soutoul, A., et al.: Astron. Astrophys. **233** (1990) 96.

91A Adams, J.H. Jr., Beahm, L.P., Tylka, A.J.: Astrophys. J. **377** (1991) 292.
91G Grigorov, N.L., Kondratyeva, M.A., Panasyuk, M.I., et al.: Geophys. Res. Lett. **18** (1991) 1959.
91S Singh, R.K., Mitra, B., Durgaprasad, N., Biswas, S., et al.: Astrophys. J. **377** (1991) 292.
93C Cummings, J.R., Cummings, A.C. , Mewaldt, R.A., et al.: Geophys. Res. Lett. **20** (1993) 2003.
95C1 Christian, E.R., Cummings, A.C., Stone, E.C.: Astrophys. J. **446** (1995) L105.
95C2 Cummings, A.C., Mewaldt, R.A., Blake, J.B., et al.: Geophys. Res. Lett. **22** (1995) 341.
95K Klecker, B., McNab, M.C., Blake, J.B., et al.: Astrophys. J. **442** (1995) L69.
95M McDonald, F.B., Lukasiak, A., Webber, W.R.: Astrophys. J. **446** (1995) L101.
95S Selesnick, R.S., Cummings, A.C., Cummings, J.R., et al.: J. Geophys. Res. **100** (1995) 9503.
96J Jokipii, J.R.: Astrophys. J. **466** (1996) L47.
96L Leske, R.A., Mewaldt, R.A., Cummings, A.C., et al.: Space Sci. Rev. **78** (1996) 149.
96M Mewaldt, R.A., Selesnick, R.S., Cummings, J.R., et al.: Astrophys. J. **466** (1996) L43.
96T Trattner, K.J., Marsden, R.G., Bothmer, V., Sanderson, T.R., Wenzel, K.-P., Klecker, B., Hovestadt, D.: Astron. Astrophys. **316** (1996) 519.
98J Jokipii, J.R., and Giacalone, J.: Space Science. Rev. **83** (1998) 123.
98K Klecker, B., Mewaldt, R.A., Bieber, J.W., et al.: Space Sci. Rev. **83** (1998) 259.
98M McDonald, F.B.: Space Sci. Rev. **83** (1998) 33.
98S Steenberg, C.D., Morall, H., McDonald, F.B.: Space Sci. Rev. **83** (1998) 269.
99F Fujii, Z., McDonald, F.B.: Adv. Space Res. **23** (1999) 437.
99L Leske, R.A., Mewaldt, R.A., Christian, E.R., et al.: Proc. 26th Int. Cosmic Ray Conf. **7** (1999) 539.
99R Reames, D.V.: Astrophys. J. **518** (1999) 473.
02C Cummings, A.C., Stone, E.C., Steenberg, C.D.: Astrophys. J. **578** (2002) 194.
02S1 Schwadron, N.A., Combi, M., Huebner, W., McComas, D.J.: Geophys. Res. Lett. **29** (2002) 1993.
02S2 Slavin, J.D., Frisch, P.C.: Astrophys. J. **565** (2002) 364.
05S Stone, E.C., Cummings, A.C., McDonald, F.B., et al.: Science **309** (2005) 2017.
07C Cummings, A.C., Stone, E.C.: Space Sci. Rev. **130** (2007) 389.
07G Grevesse, N., Asplund, M., Sauval, A.J.: Space Sci. Rev. **130** (2007) 105.
07J Jokipii, J.R., Giacalone, J., Kóta, J.: Planet. Space Sci. **55** (2007) 2267.
07S Schwadron, N.A., McComas, D.J.: Geophys. Res. Lett. **34** (2007) L14105.

4.3.6.3 Gases of non-solar origin in the Solar System

4.3.6.3.1 Introduction

The state of the undisturbed very local interstellar medium (VLISM) with its density, composition, temperature and relative velocity can be determined from measurements of interstellar absorption lines in the light of nearby stars [LB/NS VI/1, Subsection 8.4.1.2, 87C, 90F, 96L]. The Solar System is moving relative to the VLISM. While the plasma component of the VLISM is excluded from the Solar System by the interplanetary magnetic field, the neutral interstellar gas flows through the system [70B].

In the Solar System the neutral particles of the VLISM perform Keplerian trajectories under the influence of solar gravitation and radiation pressure. In the inner heliosphere the neutral gas is subject to ionization by solar ultraviolet radiation, charge exchange with solar wind ions and electron collisions. The combination of these effects results in a characteristic spatial distribution of each neutral species in the heliosphere that depends on the ionization potential, the initial velocity distribution, and radiation pressure. Schematic views of the distribution in the ecliptic plain are given for H and He in Figs. 4a and 4b, respectively. The loss processes lead to a density variation for all species, with density decreasing with decreasing radial distance from the sun. For H the radiation pressure is comparable or even exceeds the gravitation, this leading to a wake of the neutral gas in the downwind side of the sun. For He and heavier species the radiation pressure is negligible, resulting in a focused cone on the downwind side of the sun. For reviews see [72A, 74F, 77H, 90A, 90L, 90M, 04M2, 07L].

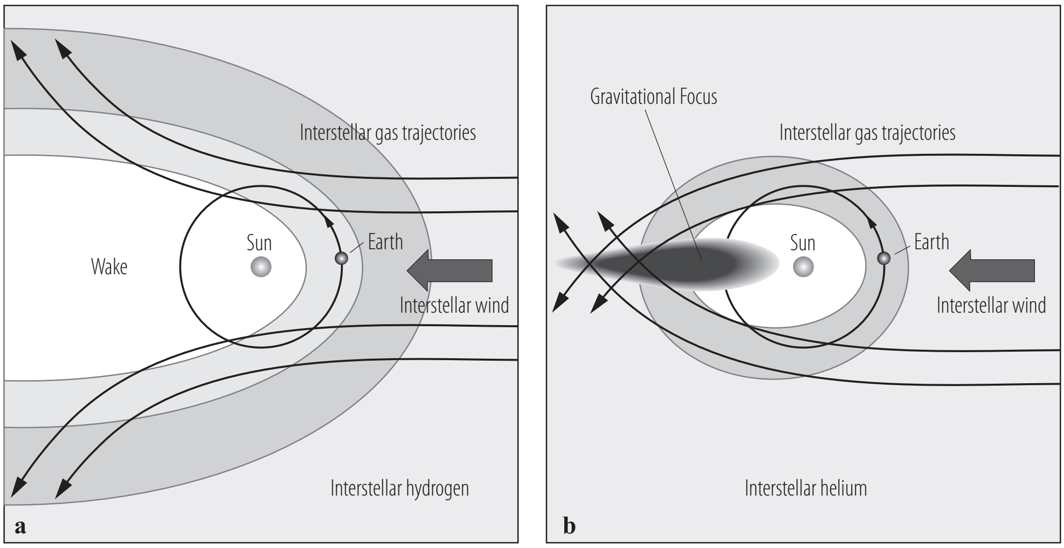

Fig. 4. Cut through the distribution of interstellar neutral gas in the inner Solar System in the ecliptic plane. (a) Distribution of neutral hydrogen: the radiation pressure of the sun dominates and a wake is created downwind of the sun. (b) Distribution of neutral helium: the solar gravitation dominates and the interstellar wind is focused on the downwind side of the sun.

4.3.6.3.2 Determination of the interstellar gas distribution in the heliosphere

The distribution of the interstellar gas flow is determined by the combination of model calculations with three independent observational techniques listed below [77H, 78T, 79W, 90L, 96R]. As a result of the comparison of the calculations with the measurements the local interstellar density n_0, temperature T_0 and velocity vector $\boldsymbol{V_0}$, with magnitude V_0, heliocentric ecliptical longitude λ and latitude β of the interstellar wind flow in the Solar System are derived. The most precise information can be derived from He because it enters the heliosphere unimpeded, different from other species as H or O that are significantly changed through charge exchange in the heliospheric interface [91F, 93R, 00M].

1) Observation of the directional distribution of backscattered light of solar emission lines.

The sky map of the scattered light is compared with the results of the model calculations of the neutral gas density distribution and the corresponding line-of-sight integral of the light emission in order to derive the VLISM parameters. This technique has been applied to H using the H I 1216 Å line [85B, 86C] and to He using the He I 584 Å line. In addition, V_0 and T_0 have been derived directly from the line profile of the scattered light for H [71B, 71T, 77A] and He [04L, 04V].

2) The observation of the spatial flux distribution of pickup ions in the solar wind from spacecraft.

After ionization in the Solar System the interstellar particles are subject to the combined forces of the interplanetary magnetic and $\boldsymbol{V_{SW}} \times \mathbf{B}$ electric fields and convected as pickup ions with the solar wind, where $\boldsymbol{V_{SW}}$ and $\boldsymbol{B}$ are the solar wind velocity and magnetic field vectors, respectively. The energy flux density of the pickup ions is proportional to the production of these ions upstream of the observer. From a spacecraft near Earth orbit the neutral gas distribution in the ecliptic, inside Earth's orbit can be measured during the course of the year, thus determining the amplitude and width of the focusing cone (Fig. 4b). This technique has been applied to He [85M, 96M, 04G1, 04M2]. The maximum velocity of pickup ions as measured on spacecraft also provides information on the velocity of the interstellar medium relative to the solar wind (V_{rel}), with a systematic annual variation from $V_{SW} + V_0$ to $V_{SW} - V_0$ for measurements in the upstream and downstream direction, respectively [99M]. Model calculations of the pickup ion distribution in the solar wind, combined with measurements of pickup H, He, O, Ne, then provide information on the parameters of the local interstellar medium [76V, 85M, 87I, 88M, 04G2].

3) Direct measurement of interstellar neutral He with the GAS experiment onboard Ulysses

The velocity and direction of the flow of the interstellar helium and its temperature and density have been derived from the measurements of the Interstellar Neutral Gas Experiment onboard Ulysses. This method combines the in-situ determination of the local flow velocity of individual neutral He atoms with model calculations to infer V_0, T_0, and n_0 outside the heliosphere [93W, 96W, 04W].

The neutral gas distribution for each species varies with the ionization rate and therefore with solar activity [87F] and the solar wind flux [85L]. Except for the focusing cone on the downwind side of the sun the interstellar gas distribution is well described by a cold gas approximation [76V, 77H, 78T]

$$N(r, \theta) = n_0/\sin\theta \{\partial b_1/\partial r \exp[-r_i\theta / b_1] + \partial b_2/\partial r \exp[-r_i(2\pi-\theta)/b_2]\} \quad (1)$$

with

$$b_{1,2} = [(r/2 \sin\theta)^2 + (1-\mu)\, GM_S / V_0^2\, r\,(1-\cos\theta)]^{1/2} \pm r / 2 \sin\theta \quad (2)$$

$$r_i = r_0^2\, \nu_{ion} / V_0 \quad (3)$$

where r is the distance from the sun, θ is the angular separation from the velocity vector of the sun with respect to the VLISM, and r_i is a characteristic penetration distance of the interstellar gas with ν_{ion} being the ionization rate at the reference distance r_0. The term GM_S / r^2 represents the gravitational acceleration by the sun and μ is the relative contribution of the radiation pressure. Ionization rates at 1 AU and the typical penetration distances r_i from the sun are compiled in Table 1 for low to moderate solar activity, for V_0 = 20 km/sec, and for various elements in the mass range hydrogen to argon.

Table 1 provides ionization rates typical for low and moderate solar activity and the resulting penetration distances for H, He, N, O, Ne, and Ar. The photoionization rates are based on photon flux densities of about 2×10^{10} photons cm^{-2} s^{-1} for 910 to 375 Å and about 3.6×10^{10} photons cm^{-2} s^{-1} for 665 to 150 Å [73B], which are appropriate for low to moderate solar activity. Most recent measurements of the solar UV flux which affects the ionization of He have confirmed that it varies linearly with the F10.7-cm solar radio flux. The photon flux density for 575 to 50 Å varies typically from 3.6×10^{10} to 5.5×10^{10} photons cm^{-2} s^{-1} for F10.7-cm radio flux densities from 0.01 to 0.02 W cm^{-2} Hz^{-1} [89F, 90O]. To adjust for varying solar activity, the UV flux densities and ionization rates may be scaled accordingly. The charge exchange rates are based on solar wind flux densities of about 3.3×10^8 particles cm^{-2} s^{-1} for H^+ and about 1.5×10^7 particles cm^{-2} s^{-1} for He^{2+}. Electron ionization rates correspond to a solar wind electron distribution which exists of a cold core component with a number density and temperature of about 6.7 cm^{-3} and 1.5×10^5 K, respectively, and a hot halo component with a density and temperature of about 0.3 cm^{-3} and 7×10^5 K, respectively (all values at the reference distance of 1 AU).

In order to include the cone structure in the model and to allow the determination of the temperature a more sophisticated model is necessary [77H, 78T, 79W]. Table 2 provides the most recent results for the VLISM parameters as derived from the combination of model calculations and the three experimental methods outlined above. A compilation of earlier results may be found in [86C, 87A]. The derived values of the results are model dependent. The uncertainties of the backscatter results depend on the uncertainties in the total intensity and the shape [88C] of the solar spectral lines. The pickup ion results and the results of the direct measurement of neutral He depend on the uncertainties of the ionization rates [88M, 96W, 04M1]. However, due to independent measurements of the solar EUV flux [04M1] and of the solar wind it was possible to considerably reduce the uncertainties of the parameters of the interstellar wind [04M2].

Table 1. Ionization rates and penetration distances from the sun

Species	Reaction	ν_{ion} [10^{-7} sec^{-1}] partial	total	r_i [AU]	Ref.
Hydrogen			7.8	5.9	
	$H + h\nu \rightarrow H^+ + e$	0.880			77H
	$H + H^+ \rightarrow H^+ + H$	6.600			77H
	$H + He^{2+} \rightarrow H^+ + He^+$	0.033			77H
	$H + e \rightarrow H^+ + 2e$	0.270			89R
Helium			0.995	0.76	
	$He + h\nu \rightarrow He^+ + e$	0.800			73B, 90R
	$He + H^+ \rightarrow He^+ + H$	0.045			90R
	$He + e \rightarrow He^+ + 2e$	0.150			89R
Nitrogen			8.8	6.6	
	$N + h\nu \rightarrow N^+ + e$	2.8			73B, 68M
	$N + H^+ \rightarrow N^+ + H$	6.0			72A
Oxygen			6.0	4.5	
	$O + h\nu \rightarrow O^+ + e$	3.3			73B
	$O + H^+ \rightarrow O^+ + H$	2.7			72A
Neon			2.93	2.2	
	$Ne + h\nu \rightarrow Ne^+ + e$	2.6			73B, 68M
	$Ne + H^+ \rightarrow Ne^+ + H$	0.33			72A
Argon			6.1	4.6	
	$Ar + h\nu \rightarrow Ar^+ + e$	2.8			73B, 68M
	$Ar + H^+ \rightarrow Ar^+ + H$	3.3			72A

The extrapolation of the measured interstellar gas parameters to the undisturbed conditions outside the Solar System depends on assumptions about the influence of the interface between the heliosphere and the interstellar medium [83R, 84F, 87B, 04I]. Depending on the fractional ionization of the interstellar medium and on charge exchange reactions in the interface, part of the neutral gas may be coupled to the interstellar plasma flow and prevented from entering the heliosphere [04I]. Table 3 summarizes the results on the density of interstellar gas inside and outside the heliosphere, taking into account the predicted filtration effect by charge exchange and electron impact ionization in the interface.

Table 2. Parameters of the interstellar wind in the heliosphere

	Method	n_0 [cm^{-3}]	T_0 [K]	V_0 [km/s]	λ [°]	β [°]	Ref.
H	Backscatter	0.03 …0.06	7000±1000	20±1	71±2	−7.5 ±3	85B
He	Backscatter	0.013±0.003	6500±2000	24.5±2	74.7±0.5	−5.7±0.5	04V
	Pickup ions	0.0154±0.0015					04G1
	Neutral gas	0.015±0.003	6300±340	26.3±0.4	74.4±0.5	−5.2±0.2	04W
	Mean	0.0148±0.002	6306±390	26.2±0.4	74.68±0.56	−5.31±0.28	04M2

with local interstellar density n_0, temperature T_0, magnitude of the velocity V_0 and heliocentric ecliptical longitude λ and latitude β of the interstellar wind flow direction.

The charge exchange between interstellar neutral and solar wind ions creates a population of neutral particles with solar wind velocity which may be used as a diagnostic of the interaction between the interstellar gas and the solar wind [90G1, 90G2, 01G].

Table 3. Density of interstellar neutral particles

	Method	Inside TS n_0 [cm^{-3}]	Filtration factor	VLISM n_0 [cm^{-3}]	Ref.
Hydrogen	Lyα Absoption	0.0575±0.0045	0.54±0.04	0.1065±0.028	95L, 04I
^{4}He	Weighted mean	0.0148±0.002	1.00	0.0148±0.002	04M2
^{3}He	Pickup ions	3.6±1.0 10^{-6}	0.94±0.023	3.8±1.1 10^{-6}	04G2
Nitrogen	Pickup ions	7.8±1.5 10^{-6}	0.78±0.08	1.1±0.2 10^{-5}	04G2, 04I
Oxygen	Pickup ions	5.3±0.8 10^{-5}	0.68±0.03	7.8±1.3 10^{-5}	04G2, 04I, 07L
Neon	Pickup ions	7.6±1.5 10^{-6}	0.88±0.04	8.6±1.7 10^{-6}	02C, 04G2
Argon	ACR	2.2±0.9 10^{-7}	0.64±0.11	3.5±1.6 10^{-7}	02C, 07L

Further indirect information on the composition of the interstellar neutral gas in the heliosphere can be obtained from the composition of the anomalous component of cosmic rays (see 4.3.6.3.2).

The gases of non-solar origin in the heliosphere strongly depend on the galactic environment. Table 2 and 3 summarize neutral particle parameters for contemporary medium conditions. However, with changing conditions in the local galactic environment, significant changes can be expected, in particular when the sun encounters regions of significantly smaller (Local Bubble) or larger densities of the local interstellar medium [06F, 06M].

References for 4.3.6.3

General References

a Physiscs of the Outer Heliosphere (Grzedzielski, S., Page, D.E., eds). COSPAR Colloquia Series 1 (1990)

b Solar Journey: The significance of our galactic environment for the Heliosphere and Earth (Frisch, P.C. ed), Springer (2006).

Special References

68M McGuire, E.J.: Phys. Rev. **175** (1968) 20.
70B Blum, P.W., Fahr, H.-J.: Astron. Astrophys. **4** (1970) 280.
71B Bertaux, J.L., Blamont, J.E.: Astron. Astrophys. **11** (1971) 200.
71T Thomas, G.E., Krassa, R.F.: Astron. Astrophys. **11** (1971) 218.
72A Axford, W.I., In: Solar Wind (Sonett, C.P., Coleman Jr., P.J., Wilcox, J.M., eds) NASA SP-308 (1972) 609.
73B Banks, P.M., Kockarts, G.: Aeronomy, Part 1, New York: Academic Press (1973).
74F Fahr, H.J.: Space Science Rev. **15** (1974) 483.
76V Vasyliunas, V.M., Siscoe G.L.: J. Geophys. Res. **81** (1976) 1247.
77A Adams, T.F., Frisch, P.C.: Astrophys. J. **212** (1977) 300.
77H Holzer, T.E.: Rev. Geophys. Space Phys. **15** (1977) 467.
78T Thomas, G.E.: Annu. Rev. Earth Planet. Sci. **6** (1978) 173.
79W Wu, F.M., Judge, D.L.: Astrophys. J. **231** (1979) 594.
83R Ripken, H.W., Fahr, H.-J.: Astron. Astrophys. **122** (1983) 181.
84F Fahr, H.J., Ripken, H.W.: Astron. Astrophys. **139** (1984) 551.
85B Bertaux, J.L., Lallement, R., Kurt, V.G., Mironova, E.N.: Astron. Astrophys. **150** (1985) 1.
85L Lallement, R., Bertaux, J.L., Kurt, V.G.: J. Geophys. Res. **90** (1985) 1413.
85M Möbius, E., Hovestadt, D., Klecker, B., et al.: Nature **318** (1985) 426.
86C Chassefiere, E., Bertaux, J.L., Lallement, R., Kurt, V.G.: Astron. Astrophys. **160** (1986) 229.
87A Ajello, J.M., Stewart, A.I., Thomas, G.E., Graps, A.: Astrophys. J. **317** (1987) 964.
87B Bleszynski, S.: Astron. Astrophys. **189** (1987) 201.

87C Cox, D.P., Reynolds, R.J.: Annu. Rev. Astron. Astrophys. **25** (1987) 303.
87F Fahr, H.J., Nass, H.-U., Rucinski, D.: Ann. Geophys. **5A** (1987) 255.
87I Isenberg, P.A.: J. Geophys. Res. **92** (1987) 1067.
88C Chassefiere, E., Dalaudier, F., Bertaux, J.-L.: Astron. Astrophys. **201** (1988) 113.
88M Möbius, E., Klecker, B., Hovestadt, D., Scholer, M.: Astrophys. Space Sci. **144** (1988) 487.
89F Feng, W., Ogawa, H.S., Judge, D.L.: J. Geophys. Res. **94** (1989) 9125.
89R Rucinski, D., Fahr, H.J.: Astron. Astrophys. **224** (1989) 290.
90A Axford, W.I.: see General references [a] p. 7.
90F Frisch, P.C.: see General references [a] p. 19.
90G1 Gruntman, M.A., Leonas, V.B., Grzedzielski, S.: see General references [a] p. 355.
90G2 Grzedzielski, S., Rucinski, D.: see General references [a] p. 367.
90L Lallement, R.: see General references [a] p. 49.
90M Möbius, E.: see General references [a] p. 345.
90O Ogawa, H.S., Canfield, L.R., McMullin, D.R., Judge, D.L.: J. Geophs. Res. **95** (1990) 227.
90R Ratkiewicz, R., Rucinski, D., Ip, W.H.: Astron. Astrophys. **230** (1990) 227.
91F Fahr, H.J.: Astron. Astrophys. **241** (1991) 251.
93R Rucinski, D., Fahr, H.J., Grzedzielski, S.: Planet. Space Sci. **41** (1993) 773.
93W Witte, M., Rosenbauer, H., Banaszkiewicz, M.: Adv. Space Res. **13(6)** (1993) 121.
95L Linsky, J.L., Diplas, A., Wood, B.E., et al.: Astrophys. J. **451** (1995) 335.
96L Lallement, R.: Space Science Rev. **78** (1996) 361.
96M Möbius, E.: Space Science Rev. **78** (1996) 375.
96R Rucinski, D., Bzowski, M.: Space Science Rev. **78** (1996) 265.
96W Witte, M., Banaszkiewicz, M., Rosenbauer, H.: Space Science Rev. **78** (1996) 289.
99M Möbius, E., Litvinenko, Y., Grünwaldt, H., et al.: Geophys. Res. Lett. **26** (1999) 3181.
00M Müller, H.R., Zank, G.P., Lipatov, A.S.: J. Geophys. Res. **105** (2000) 27419.
01G Gruntman, M.: J. Geophys Res. **196** (2001) 8205.
02C Cummings, A.C., Stone, E.C., Steenberg, C.D.: Astrophys. J. **578** (2002) 194.
04G1 Gloeckler, G., Möbius, E., Geiss, J., et al.: Astron. Astrophys. **426** (2004) 845.
04G2 Gloeckler, G., Geiss, J.: Adv. Space Res. **34** (2004) 53.
04I Izmodenov, V., Malama, Y., Gloeckler, G., Geiss, J.: Astron. Astrophys. **414** (2004) L29.
04L Lallement, R., Raymond, J.C., Bertaux, J.-L., et al.: Astron. Astrophys. **426** (2004) 867.
04M1 McMullin, D.R., Bzowski, M., Möbius, E., et al.: Astron. Astrophys. **426** (2004) 885.
04M2 Möbius, E., Bzowski, M., Chalov, S., et al.: Astron. Astrophys. **426** (2004) 897.
04V Vallerga, J., Lallement, R., Raymond, J., et al.: Astron. Astrophys. **426** (2004) 855.
04W Witte, M.: Astron. Astrophys. **426** (2004) 835.
06F Frisch, P.C., Slavin, J.D.: see General references [b] p. 133.
06M Möbius, E., Bzowski, M., Müller, H.-R., Wurz, P.: see General references [b] p. 209.
07L Lallement, R.: Space Science Rev. **130** (2007) 341.